JPET Fast Forward. Published on October 25, 2018 as DOI: 10.1124/jpet.118.252809
This article has not been copyedited and formatted. The final version may differ from this version.

Title Page

Title:

Single dose of polyanhydride particle-based vaccine generates potent antigen-specific antitumor immune responses

Authors:

Emad I. Wafa, Sean M. Geary, Kathleen A. Ross, Jonathan T. Goodman, Balaji Narasimhan, Aliasger K. Salem

Affiliations:

Department of Pharmaceutical Sciences and Experimental Therapeutics, College of Pharmacy, University of Iowa, Iowa City, IA 52242, USA (E.I.W., S.M.G., A.K.S.); Department of Chemical and Biological Engineering, College of Engineering, Iowa State University, Ames, IA 50011, USA (K.A.R., J.T.G., B.N.); Nanovaccine Institute, Iowa State University, Ames, IA 50011 and University of Iowa, Iowa City, IA 52242, USA (K.A.R., B.N., A.K.S.)

Downloaded from jpet.aspetjournals.org at ASPET Journals on April 18, 2024

JPET Fast Forward. Published on October 25, 2018 as DOI: 10.1124/jpet.118.252809
This article has not been copyedited and formatted. The final version may differ from this version.

Running Title Page

Running Title:

Single dose of polyanhydride particle-based vaccine

Corresponding author:

Aliasger K. Salem, Ph.D.
Department of Pharmaceutical Sciences and Experimental Therapeutics
College of Pharmacy, University of Iowa
115 S. Grand Avenue, S228 PHAR
Iowa City, IA 52242
Phone: 319 335-8810
FAX: 319 335-9349
aliasger-salem@uiowa.edu

Number of text pages: **20**

Number of tables: **1**

Number of figures: **9**

Numbers of references: **44**

Number of words in the Abstract (≤250): **222**

Number of words in the Introduction (≤750): **750** (including references)

Number of words in the Discussion (≤1500): **1163** (including references)

Downloaded from jpet.aspetjournals.org at ASPET Journals on April 18, 2024

JPET Fast Forward. Published on October 25, 2018 as DOI: 10.1124/jpet.118.252809
This article has not been copyedited and formatted. The final version may differ from this version.

List of nonstandard abbreviations:

APCs	antigen presenting cells
BCA	bicinchoninic acid
BMDCs	bone marrow-derived dendritic cells
C6	coumarin-6
CPH	1,6-bis(*p*-carboxyphenoxy) hexane
CPTEG	1,8-bis(*p*-carboxyphenoxy)-3,6-dioxaoctane
DCs	dendritic cells
OVA	ovalbumin
PBLs	peripheral blood lymphocytes
PBS	phosphate buffered saline
PDI	polydispersity index
PVA	poly(vinyl alcohol)
SEM	scanning electron microscope
TLRs	Toll-like receptors

Recommended section assignment:

Immunopharmacology

Downloaded from jpet.aspetjournals.org at ASPET Journals on April 18, 2024

JPET Fast Forward. Published on October 25, 2018 as DOI: 10.1124/jpet.118.252809
This article has not been copyedited and formatted. The final version may differ from this version.

Abstract

There are many factors affecting vaccine efficacy. One of the most salient of these is the frequency and intervals of vaccine administration. In this study, vaccine administration modality for a recently reported polyanhydride-based vaccine formulation, shown to generate antitumor activity, was assessed. Polyanhydride particles encapsulating ovalbumin (OVA) were prepared using a double emulsion technique and subcutaneously delivered to mice either as a single dose or as prime-boost vaccine regimens where two different time intervals between prime and boost were assessed (7 or 21 days). This was followed by measuring cellular and humoral immune responses, and subsequently challenging the mice with a lethal dose of E.G7-OVA cells to evaluate tumor protection. Interestingly, a single dose of the polyanhydride particle-based formulation induced sustained OVA-specific cellular immune responses just as effectively as the prime-boost regimens. In addition, mice receiving a single dose vaccine had a similar level of protection against tumor challenge compared to mice administered prime-boosts. In contrast, measurements of OVA-specific IgG antibody titers indicated that a booster dose was required to stimulate strong humoral immune responses since it was observed that mice administered with a prime-boost vaccine had significantly higher OVA-specific IgG_1 serum titers than mice administered with a single dose. These findings indicate that the requirement for a booster dose using these particles appears unnecessary for the generation of effective cellular immunity.

Keywords: Polyanhydride-based particles, antitumor immune response, single dose cancer vaccine, sustained release, vaccine administration regimen.

Downloaded from jpet.aspetjournals.org at ASPET Journals on April 18, 2024

JPET Fast Forward. Published on October 25, 2018 as DOI: 10.1124/jpet.118.252809
This article has not been copyedited and formatted. The final version may differ from this version.

1. Introduction

Despite recent biotechnological and therapeutic advances, cancer continues to be a challenging health problem (Garcia-Cremades et al., 2017; Siegel et al., 2017; Gomez de Cedron et al., 2018; Wang et al., 2018). With many cancer types being refractory to conventional chemotherapy and with the complication that chemotherapeutics are often limited in their efficacy due to a steep dose-response relationship and narrow therapeutic window (Paci et al., 2014; Alfarouk et al., 2015), alternative, or at least adjuvanted, therapeutic strategies are required. An alternative approach that has demonstrated considerable promise in preclinical studies is the use of cancer vaccines capable of generating tumor-specific adaptive immune responses (Andersen et al., 2006; Martinez-Lostao et al., 2015). Adaptive immune responses can be delineated as humoral (antibody-mediated) or cellular (involving $CD8^+$ T lymphocytes; often referred to as cytotoxic T lymphocytes (CTLs)). Of these two types of responses, cellular immunity is considered the more important in the context of affecting antitumor potency, particularly for tumor antigens that are not expressed on the tumor cell surface in their native form(s). Thus, generating tumor-specific CTLs has been the primary focus of clinical oncoimmunologists due to the ability of CTLs to target tumor antigens regardless of where the antigens localize to upon expression (Maher and Davies, 2004; Zhou et al., 2016). Specifically, it is likely that tumor-antigen-specific humoral immune responses are only effective against tumors that express native tumor antigens on the tumor cell surface whilst CTLs can target all tumor antigens expressed by tumors as long as the tumor cells express MHC class I and that the relevant epitope is appropriately processed and presented (Colombo et al., 2000; Andersen et al., 2006; Reuschenbach et al., 2009; Blum et al., 2013).

For successful vaccination, vaccine efficacy and safety are important aspects (Lahariya, 2016). Factors affecting vaccine efficacy, potency, and duration of immunity are

Downloaded from jpet.aspetjournals.org at ASPET Journals on April 18, 2024

JPET Fast Forward. Published on October 25, 2018 as DOI: 10.1124/jpet.118.252809
This article has not been copyedited and formatted. The final version may differ from this version.

manifold. These factors can be generally classified into three groups: (i) vaccinee (host) factors such as age, gender, and presence of co-morbidity, (ii) vaccine design/formulation parameters, including composition (+/-adjuvant), chemical, and physical properties, and (iii) vaccine delivery regimens, such as mode of delivery, dose, and frequency (Zhang et al., 2015). Variable parameters of vaccine delivery regimens, such as the number and timing of vaccine doses, are critically important factors to be considered in order to achieve optimal vaccine efficacy. While a single dose of a certain vaccine formulation may confer an enduring immunity, a single dose of a different vaccine formulation may provide protection for only a short duration and therefore may require additional dose(s) (boosters) to enhance immunopotency for longer periods (Siegrist, 2013). This may be at least partially due to the fact that different vaccine delivery vehicles can significantly differ in their release profiles with respect to their antigenic cargo from periods of days to months (Jain et al., 2005). In this regard, sustained release formulations can provide prolonged immunostimulation and induce long-lasting immune responses (Irvine et al., 2013). Since there is limited data adequately documenting the association between specific particle-based cancer vaccine regimens and the resultant qualitative and quantitative antitumor immune responses (i.e., frequencies of antigen-specific CTLs), this work focused on assessing the administration modality of a relatively new particle-based cancer vaccine formulation.

Compared to soluble antigen delivery, particulate antigen delivery platforms targeting antigen presenting cells (APCs) have a dramatic effect on immunogenicity as shown in preclinical studies (Joshi et al., 2013; Ahmed et al., 2014; Geary et al., 2015; de Barros et al., 2017; Fontana et al., 2017). In this study, ovalbumin (OVA), a model tumor antigen, was loaded into a particle-based vaccine formulation and delivered subcutaneously either as a single dose or as prime-boost vaccine regimens with distinct

Downloaded from jpet.aspetjournals.org at ASPET Journals on April 18, 2024

JPET Fast Forward. Published on October 25, 2018 as DOI: 10.1124/jpet.118.252809
This article has not been copyedited and formatted. The final version may differ from this version.

time intervals. The main objective of our current study was to assess the immune potency of these different vaccine administration regimes using a recently reported polyanhydride-based cancer vaccine formulation (Wafa et al., 2017). Formulations derived from polyanhydride polymers have shown promise as biocompatible and biodegradable polymers (Roy et al., 2016), and have been used in marketed controlled-release medical products such as Gliadel® (polyanhydride-based wafer containing carmustine for treating glioblastoma multiforme) and Septacin™ (polyanhydride-based beads loaded with gentamycin for treating osteomyelitis) (Li et al., 2002; Jain et al., 2005; Perry et al., 2007). In addition, polyanhydride particles have been reported to possess immunostimulatory properties by triggering Toll-like receptor (TLR) mediated signaling in dendritic cells (DCs) (Tamayo et al., 2010). Here, our goal was to determine the effects on antigen-specific immune responses and tumor growth of varying the prime-boost regimen of an antigen-loaded polyanhydride particle formulation.

2. Materials and Methods

2.1 Particle preparation and characterization

2.1.1 Preparation of empty, OVA-, and coumarin-loaded polyanhydride particles

Monomers of 1,8-bis(*p*-carboxyphenoxy)-3,6-dioxaoctane (CPTEG) and 1,6-bis(*p*-carboxyphenoxy) hexane (CPH) were copolymerized in a 20:80 molar ratio (**Figure 1**) via melt polycondensation, as previously described (Wafa et al., 2017). The purity, composition, and molecular weight of the polymer were verified with ^{1}H nuclear magnetic resonance (Varian VXR-300 MHz, Varian Inc., Palo Alto, CA) and found to be consistent with previous publications (Torres et al., 2007; Wafa et al., 2017). Polyanhydride particles encapsulating OVA were prepared using a water-in-oil-in-water double emulsion solvent-evaporation technique, as described previously (Wafa et al., 2017). In brief, 75 µL of 1%

Downloaded from jpet.aspetjournals.org at ASPET Journals on April 18, 2024

JPET Fast Forward. Published on October 25, 2018 as DOI: 10.1124/jpet.118.252809
This article has not been copyedited and formatted. The final version may differ from this version.

w/v poly(vinyl alcohol) (PVA) (Mowiol® 8-88, Sigma-Aldrich, Allentown, PA) containing 3 mg of chicken egg white OVA (Sigma-Aldrich, St. Louis, MO) was sonicated for 30 seconds into 1.5 mL of dichloromethane (Sigma-Aldrich) containing 200 mg of 20:80 CPTEG:CPH copolymer. The obtained primary emulsion was immediately emulsified into 8 mL of 1% w/v PVA solution (under the same previous conditions). The resulted emulsion was instantly added to 22 mL of 1% w/v PVA solution and stirred in a fume hood for 2 hrs to allow evaporation of dichloromethane. After 2 hrs, particles were collected at 2880 x*g*, for 5 min. The obtained particles were washed twice with sterile nanopure water. The particle suspension was frozen at –80°C for 1 hr and subsequently lyophilized for 24 hrs. Finally, particles were collected in a sealed container and stored at –20°C until being used. Empty (i.e., no protein) polyanhydride particles, used to assess the stimulatory effect of polyanhydride particles on DCs, were also prepared using the same method, except that the internal aqueous phase (i.e., 1% w/v PVA) had no OVA. To evaluate the uptake efficiency by DCs, a hydrophobic model drug coumarin-6 (C6) (MW: 350.43 g/mol) (Sigma-Aldrich) was loaded into the particles using the same technique as described above with only one exception: 200 µg of C6 was added to the oil phase (i.e., dichloromethane) into which the polymer was already dissolved. C6 is a photoluminescent compound, and it has been widely used to perform cell uptake studies (Behroozi et al., 2018; Dilnawaz and Sahoo, 2018; Tian et al., 2018).

2.1.2 Particle characterization

Polyanhydride particles were characterized in terms of size, shape, and surface charge. Suspensions of particles in nanopure water were used to measure particle properties. Size distribution and surface charge were measured using a Zetasizer Nano ZS instrument (Malvern, Southborough, MA), as described previously (Wafa et al., 2017). The size was measured using a dynamic light scattering at a backscattering angle of 173°

Downloaded from jpet.aspetjournals.org at ASPET Journals on April 18, 2024

JPET Fast Forward. Published on October 25, 2018 as DOI: 10.1124/jpet.118.252809
This article has not been copyedited and formatted. The final version may differ from this version.

whilst the net charge on particles' surface was measured using laser doppler electrophoresis at a forward-scattering beam angle of 13°. Particles were also examined for their shape and surface morphology using a Hitachi S-4800 scanning electron microscope (SEM) (Hitachi High-Technologies, Ontario, Canada), as described previously (Wafa et al., 2017). Silicon wafer chips (Ted Pella Inc., Redding, CA) doped with polyanhydride particles and mounted on a flat SEM pin stub were coated with gold-palladium using an argon beam K550 sputter coater (Emitech Ltd., Kent, U.K.) for 3 min. Subsequently, SEM photomicrographs were captured at 2 kV accelerating voltage and images were processed using ImageJ (National Institutes of Health, Bethesda, MD).

2.2 Quantification of OVA-loaded and C6-loaded polyanhydride particles

OVA content in polyanhydride particles was measured using a bicinchoninic acid (BCA) protein assay, as described previously (Wafa et al., 2017). In brief, OVA-loaded particles were treated with 1 mL of 0.2 N NaOH and incubated overnight in an orbital incubator shaker (New Brunswick Scientific Co. Inc., Edison, NJ) set at 37°C and 300 rpm. A Micro BCA™ Protein Assay Kit (Thermo Fisher Scientific, Rockford, IL) was used to determine the protein concentration in the samples after being neutralized by 0.3 N HCl. Subsequently, samples were stepwise diluted using phosphate buffered saline (PBS) (Sigma-Aldrich) in 96-well plate (Celltreat, Pepperell, MA) and incubated with Micro BCA™ reagents for 2 hrs at 37°C. After incubation, the absorbance of the solutions at 562 nm was measured using a SpectraMax® Plus 384 microplate reader (Molecular Devices, Sunnyvale, CA). Bovine serum albumin standard solution was used to generate the standard curve under the same conditions and three replicates of all samples were assayed. The results were expressed as micrograms of OVA per milligram of particles, as described in equation (1). The percent encapsulation efficiency was expressed as the percentage of the total OVA entrapped to the amount of OVA used to prepare the

Downloaded from jpet.aspetjournals.org at ASPET Journals on April 18, 2024

JPET Fast Forward. Published on October 25, 2018 as DOI: 10.1124/jpet.118.252809
This article has not been copyedited and formatted. The final version may differ from this version.

formulation, as described in equation (2). Additionally, the amount of C6 entrapped in polyanhydride particles was quantified by measuring the fluorescence intensity. Briefly, C6-loaded polyanhydride particles were dissolved in chloroform (Fisher Scientific, Fair Lawn, NJ) and the fluorescence intensity of C6 was measured at excitation/emission wavelengths of 405/495 nm, using a SpectraMax® M5 microplate reader (Molecular Devices). A standard curve of C6 in chloroform was also generated. All samples were run in triplicate, and the mean with standard deviation (SD) were reported. Similarly, the loading capacity and encapsulation efficiency was calculated as described in equations (1) and (2).

$$\text{Loading capacity} = \frac{\text{OVA (or C6) concentration} \times \text{volume of solution}}{\text{weight of particles}} \qquad (1)$$

$$\text{Encapsulation efficiency} = \frac{\text{yield of particles} \times \text{loading capacity}}{\text{initial weight of OVA (or C6)}} \times 100 \qquad (2)$$

2.3 *In vitro* release of OVA

Samples of 20:80 CPTEG:CPH polyanhydride particles encapsulating OVA (≈ 30 mg) were dispersed into 5 mL of PBS and incubated in the orbital incubator shaker set at 37°C and 300 rpm for one month. The amount of OVA released from particles into the medium was measured at predetermined time intervals (1 hr, 12 hrs, 1, 2, 4, 7, 10, 14, 20, and 30 days) and aliquots (0.5 mL) of the release medium was withdrawn and the total volume was replenished by fresh PBS at each time interval. Supernatants were stored at –20°C until OVA content was measured by the BCA protein assay (as described above). The experiment was performed in triplicate, and the results were expressed as the mean of cumulative OVA-release into PBS determined as a function of time ± SD.

Downloaded from jpet.aspetjournals.org at ASPET Journals on April 18, 2024

JPET Fast Forward. Published on October 25, 2018 as DOI: 10.1124/jpet.118.252809
This article has not been copyedited and formatted. The final version may differ from this version.

2.4 *In vitro* experiments with DCs

Quantitative and qualitative cellular uptake and subsequent stimulatory effects of polyanhydride particles on DCs were studied. DCs were derived from the bone marrow of C57BL/6J mice as previously described (Liu et al., 2018). Briefly, bone marrow cells were extracted from the femur and tibia, and were grown on Bacteriological Petri dishes in Roswell Park Memorial Institute medium (RPMI 1640) supplemented with: 10 mM HEPES buffer, 1 mM sodium pyruvate, 0.1 mM minimal essential medium nonessential amino acids MEM-NEAA, 2 mM GlutaMAX (Life Technologies, Grand Island, NY), 50 mM 2-mercaptoethanol (Sigma), 50 ng/mL gentamicin sulfate (IBI Scientific, Peosta, IA), 10% fetal bovine serum (Atlanta Biologicals, Flowery Branch, GA), and 20 ng/mL of murine granulocyte-macrophage colony stimulating factor (GM-CSF) (PeproTech, Rocky hill, NJ), in a humidified incubator at 37°C containing 5% CO_2. Bone marrow-derived DCs (BMDCs) were harvested at day 10 of culture, seeded in 12-well Cellstar plates (Greiner Bio-One, Germany) at a density of 3 x 10^5 cells/well, and incubated for 6 hrs prior to treatment. This was followed by adding polyanhydride particles (delivering a total dose of 0.02 μg C6-loaded or empty particles at equivalent amount) and incubating for either 1 to 4 hrs for uptake studies or 24 hrs to assess BMDC activation and maturation. After incubation with designated treatments, cells were collected (without using trypsin; instead vigorous flushing was implemented) and centrifuged (230 x*g*) for 5 min at 4°C. In the DC stimulation experiment, cell culture supernatants were harvested and assayed for IL-10 and IL-12p70 levels using a cytokine specific mouse enzyme-linked immune-sorbent assay (ELISA) kit (Thermo Fisher Scientific, San Diego, CA), as per manufacturer's instructions. Cells treated with empty particles were stained with anti-CD11c-fluorescein isothiocyanate (FITC) and either anti-CD80-PE or anti-CD86-PE (eBioscience, San Diego, CA) using a standard direct immunofluorescence method. Controls involved staining DCs with FITC-

Downloaded from jpet.aspetjournals.org at ASPET Journals on April 18, 2024

JPET Fast Forward. Published on October 25, 2018 as DOI: 10.1124/jpet.118.252809
This article has not been copyedited and formatted. The final version may differ from this version.

or PE-conjugated isotype matched negative control antibodies. All cell samples (including quantitative uptake study) were run through a BD FACScan flow cytometer (Becton, Dickinson, Franklin Lakes, NJ) in triplicate and data were analyzed with FlowJo software (Tree Star, Ashland, OR). Additionally, the uptake of C6-loaded polyanhydride particles was examined qualitatively using Leica TCS SP8 STED confocal laser scanning microscope (Leica Microsystems Inc., Buffalo Grove, IL). Briefly, BMDCs were seeded at a density of $1x10^5$ cells/well (in supplemented medium) in a 4-well Nunc™ Lab-Tek™ Chamber glass slide system (Nunc, Rochester, NY) coated with poly-L-lysine hydrobromide (MW: 30,000 – 70,000) (Sigma) to promote DC attachment and incubated overnight in a well-controlled environment at 37°C with 5% CO_2. This was followed by adding polyanhydride particles (delivering a total dose of 0.02 µg C6), leaving untreated cells as a control, and incubating for 4 hrs. After incubation, the medium was removed, and the cells were washed with prewarmed (to 37°C) 1X Hank's Balanced Salt Solution (HBSS) (Life Technologies). Subsequently, specimens were stained with CellMask Orange plasma membrane stain, Texas Red-X phalloidin, and ProLong Gold antifade reagent DAPI (Life Technologies, Eugene, Oregon), respectively, as per the manufacturer's instructions. The specimens were visualized using the confocal laser scanning microscope, and the images were processed with ImageJ-based Fiji software.

2.5 Animal studies

2.5.1 Mouse strains

A murine tumor model was used for the evaluation of prophylactic cancer vaccine formulations. Wild-type female C57BL/6J mice (8 – 10 weeks of age) were purchased from Jackson Laboratories (Bar Harbor, ME). Animals were housed at the Medical Laboratories at the University of Iowa and kept on a daily 12 hr light/12 hr dark cycle. All animal

Downloaded from jpet.aspetjournals.org at ASPET Journals on April 18, 2024

JPET Fast Forward. Published on October 25, 2018 as DOI: 10.1124/jpet.118.252809
This article has not been copyedited and formatted. The final version may differ from this version.

experiments were performed in accordance with the University of Iowa guidelines for the care and use of laboratory animals.

2.5.2 Vaccination

To assess the polyanhydride vaccine *in vivo*, 40 mice were randomly divided into four groups and treated with subcutaneous (rear dorsal flank) injections using the following groups (n=10 mice per group): (I) naïve (i.e., unvaccinated), (II) single dose (primed on day 0 only), (III) prime-boost (days 0/7), and (IV) prime-boost (days 0/21). Prepared polyanhydride particles were dispersed in 1X Dulbecco's PBS (DPBS, pH 7.4) solution (Life Technologies) immediately prior to vaccination. Mice in group II received a single dose of 50 μg OVA while mice in groups III and IV received 2 doses of 50 μg OVA (i.e., prime-boost). On days 14 and 28 post-prime vaccination, tumor-specific $CD8^+$ T cells were measured in the peripheral blood harvested through submandibular bleeds. On day 28 post-prime vaccination, tumor-specific IgG_1 and IgG_{2C} antibody titers were measured in the serum harvested through submandibular bleeds. A week later, mice were challenged with tumor cells.

2.5.3 Assessment of vaccine-induced antitumor immune responses

2.5.3.1 Cell-mediated immunity

Using a submandibular bleeding technique, approximately 180 μL of mouse peripheral blood was collected into tubes containing 3 mL of ACK (ammonium-chloride-potassium) red blood cell lysing buffer, and the samples were incubated at room temperature for 5 min. After incubation, peripheral blood lymphocytes (PBLs) were washed twice with complete medium using Eppendorf Centrifuge 5804-R set at 230 x*g*, 4°C, for 5 min. Then, PBLs were resuspended in 150 μL of ice cold PBS (containing 5% fetal bovine serum and 0.1% sodium azide: FACS buffer) and transferred to v-bottomed

Downloaded from jpet.aspetjournals.org at ASPET Journals on April 18, 2024

JPET Fast Forward. Published on October 25, 2018 as DOI: 10.1124/jpet.118.252809
This article has not been copyedited and formatted. The final version may differ from this version.

96-well plates (Corning, Kennebunk, ME) on a bed of ice (as with all subsequent incubations). This was followed by centrifugation (as per the conditions described above), supernatants were discarded, and PBLs were resuspended in 50 µL of anti-mouse CD16/CD32 Fc receptor block (clone 93) (eBioscience) in FACS buffer, and incubated for 15 min. Subsequently, 50 µL of H-2Kb SIINFEKL class I iTAg™ MHC tetramer (Kb-OVA_{257}) labeled with phycoerythrin (PE) (MBLI, Woburn, MA), diluted 1/100 in FACS buffer was added in dark and samples were incubated for 30 min. After incubation, 100 µL of a mixture of fluorescein isothiocyanate (FITC)-labeled rat anti-mouse CD8 (1 µg/mL) and PE-Cy5-labeled hamster anti-mouse CD3 (eBioscience) (1 µg/mL) antibodies in FACS buffer was added in dark and incubated for 20 min. After incubation, PBLs were washed twice with FACS buffer to remove the unbound antibodies. Subsequently, 100 µL of 1X BD Cytofix/Cytoperm solution (BD Biosciences, San Jose, CA) was added and incubated for 10 min in the dark, then 100 µL of perm/wash buffer (BD Biosciences) was added, followed by centrifugation for 15 min at 660 x*g* and 4°C. Finally, PBLs were resuspended in FACS buffer, and samples were acquired using a BD FACScan flow cytometer and analyzed with FlowJo software. Results were expressed as percentage of total $CD3^+$ $CD8^+$ T lymphocytes in peripheral blood that were positive for tetramer staining.

2.5.3.2 Levels of OVA-specific antibody

The titers of tumor-specific IgG antibodies, IgG_1 and IgG_{2C}, were measured using ELISA as described previously (Wafa et al., 2017). In brief, mice were bled from the submandibular area, and to harvest sera, blood samples were incubated at room temperature for 1 hr. After incubation, blood clots were removed using clean tweezers and the samples were centrifuged for 10 min using an Eppendorf Centrifuge 5804-R set at 3,000 x*g* and 4°C. Supernatants (sera) were collected and stored at –80°C until use. In the meanwhile, Immulon® 2HB flat-bottom microtiter 96-well plates (Thermo Fisher

Downloaded from jpet.aspetjournals.org at ASPET Journals on April 18, 2024

JPET Fast Forward. Published on October 25, 2018 as DOI: 10.1124/jpet.118.252809
This article has not been copyedited and formatted. The final version may differ from this version.

Scientific) were coated with 100 µL of PBS containing 0.5 µg OVA. Using OVA-coated plates and PBS containing 0.05% v/v tween-20 (Sigma-Aldrich), sera samples were serially diluted and incubated overnight at room temperature. This was followed by incubation for 3 hrs at room temperature with either goat anti-mouse IgG_1 (or goat anti-mouse IgG_{2C}) antibody conjugated with alkaline phosphatase (Southern Biotech, Birmingham, AL). Subsequently, 100 µL of *p*-nitrophenylphosphate (*p*NPP) in TRIS buffer (Sigma-Aldrich) was added in the dark. After 30 min, the absorbance was measured at 405 nm using a SpectraMax® Plus 384 microplate reader. To remove any proteins or antibodies that were not specifically bound, plates were washed three times with 150 µL of PBS/tween-20 solution between all reagent addition steps. The reciprocal of mouse sera dilution (highest dilution at which the absorbance was three-times greater than those of negative control) was reported as serum antibody titer.

2.5.4 Tumor challenge

Five weeks post-prime vaccination, all mice were subcutaneously challenged with $2x10^6$ E.G7-OVA cells, purchased from American Type Culture Collection (ATCC®, Manassas, VA), suspended in 100 µL of sterile 1X DPBS. Cells were injected contralaterally to the vaccination site. Tumor progression was monitored regularly over time for the subsequent two months (using a digital caliper) and tumor volumes were calculated as described in equation (3). To minimize pain and discomfort, mice were euthanized when the tumor size exceeded 20 mm at the largest diameter or 10 mm in height.

$$\text{Tumor volume} = \text{diameter}_1\ (\text{mm}) \times \text{diameter}_2\ (\text{mm}) \times \text{height}\ (\text{mm}) \times \frac{\pi}{6} \qquad (3)$$

Downloaded from jpet.aspetjournals.org at ASPET Journals on April 18, 2024

JPET Fast Forward. Published on October 25, 2018 as DOI: 10.1124/jpet.118.252809
This article has not been copyedited and formatted. The final version may differ from this version.

2.5.5 Statistical analysis

Data were initially analyzed by one-way analysis of variance (ANOVA) using F-test which was followed by a Tukey's multiple comparison test to compare all pairs of treatments. Initial analysis of survival data was performed by log-rank (Mantel-Cox) test using GraphPad-Prism 7 (GraphPad Software, La Jolla, CA). Using SAS 9.4 (SAS Institute Inc., Cary, NC), further statistical analysis was made by pairwise comparisons and data were analyzed using log-rank test (Tukey-Kramer adjusted). In all tests, differences were considered statistically significant when $p<0.05$.

3. Results

3.1 Properties of polyanhydride particles

All 20:80 CPTEG:CPH particle formulations were prepared by a double emulsion method and had an average diameter of less than 1 μm (**Table 1**). In addition, particles exhibited a narrow size distribution with an average PDI value of < 0.2. Also, particles possessed a negative surface charge regardless of payload as indicated by the average zeta potential measurements. The loading capacity of OVA was low, and the encapsulation efficiency of OVA was only 28% whilst the loading capacity of C6 was relatively high (>70%). The low encapsulation efficiency of water-soluble OVA was expected since 20:80 CPTEG:CPH is a hydrophobic copolymer as indicated by its chemistry and as demonstrated by the high contact angle (Θ) between water droplets and polymer, as previously reported (Θ>90°) (Wafa et al., 2017). The analysis of SEM photomicrographs revealed that particles were spherical in shape and possessed smooth surfaces (**Figure 2.1**). *In vitro* release kinetics of OVA from polyanhydride particles showed a rapid burst release phase followed by a slower sustained release phase (**Figure 2.2 A**). By day 30, the cumulative release of OVA from 20:80 CPTEG:CPH particles had

Downloaded from jpet.aspetjournals.org at ASPET Journals on April 18, 2024

JPET Fast Forward. Published on October 25, 2018 as DOI: 10.1124/jpet.118.252809
This article has not been copyedited and formatted. The final version may differ from this version.

reached 50%. Subsequent to the burst release phase, the release of OVA approximated to zero order kinetics (**Figure 2.2 B**).

3.2 *In vitro* experiments with BMDCs

BMDCs were harvested at day 10 of culture, at which point nearly 90% of the cells were CD11c positive as analyzed by the BD FACScan flow cytometer (data not shown). Results of surface staining of BMDCs revealed that polyanhydride particles promoted the upregulation of both CD80 and CD86 to levels significantly greater than untreated BMDCs (t-test, $p<0.001$) (**Figure 3.1 A**). This further demonstrates that polyanhydrides possess self-adjuvanting properties. In addition, it was observed that polyanhydride particles could induce IL-12p70 secretion to a greater extent than IL-10 secretion (t-test, $p<0.001$), and it was found that BMDCs exposed to polyanhydride particles produced significantly high concentrations of IL-10 and IL-12p70 compared to untreated BMDCs (t-test, $p<0.001$) (**Figure 3.1 B**). Cellular uptake studies indicated that polyanhydride particles were readily and efficiently internalized by DCs as demonstrated by the significant shift in the median fluorescence intensity (**Figure 3.1 C**), and the uptake efficiency at 4 hrs was significantly greater than at 1 hr (t-test, $p<0.001$). The quantitative uptake results were supported by the confocal microscopy images, where it was evident that each DC was able to internalize several particles (**Figure 3.2**).

3.3 Assessment of immunogenicity of OVA-loaded 20:80 CPTEG:CPH polyanhydride particles

Immunocompetent mice were vaccinated with a single dose, a prime-boost (with a 7 day interval), or a prime-boost (with a 21 day interval) of OVA-loaded 20:80 CPTEG:CPH polyanhydride particles. The percentage of OVA-specific $CD8^+$ T cells in the peripheral blood measured two weeks post-prime immunization was found to be increased in mice

Downloaded from jpet.aspetjournals.org at ASPET Journals on April 18, 2024

JPET Fast Forward. Published on October 25, 2018 as DOI: 10.1124/jpet.118.252809
This article has not been copyedited and formatted. The final version may differ from this version.

administered a single dose vaccine compared to naïve mice, whilst mice receiving the prime-boost (days 0/7) regimen demonstrated increased, but not significantly, percentages of OVA-specific $CD8^+$ T cells in the peripheral blood when compared to naïve mice (**Figure 4.1 A**). On day 28 post-prime immunization, it was found that the percentage of OVA-specific $CD8^+$ T cells in mice receiving the single dose and prime-boost (day 0/7) regimens were similar to those obtained on day 14. In addition, administering a booster immunization on day 21 did not have a significant impact on OVA-specific $CD8^+$ T cell levels when compared to that induced by the single dose formulation (**Figure 4.1 B**). In contrast, humoral OVA-specific immune responses, particularly IgG_1 titers, were observed to significantly improve upon administration of a booster dose either 7 or 21 days post prime as evidenced by serum titers two orders of magnitude higher than that obtained in sera of mice receiving a single dose (**Figure 4.2**).

3.4 Evaluation of tumor progression and survival

Five weeks (day 35) post-prime vaccination, mice were challenged with a lethal dose of OVA-expressing E.G7 cells, and tumor growth and survival were subsequently recorded. As expected, naïve mice had tumors that grew rapidly compared to vaccinated mice (**Figure 5.1 A to D**). The vaccine regimen study with 20:80 CPTEG:CPH particles encapsulating OVA showed that all vaccinated mice had slow to no tumor growth in comparison to unvaccinated mice during the first 18 days post-tumor challenge. The average tumor volume, as illustrated in **Figure 5.1 E,** supports this observation where the average tumor volume curves of vaccinated mice were significantly below than that of naïve mice as demonstrated by the one-way ANOVA performed on day 16 data ($p<0.05$). Furthermore, all vaccine regimens led to 30 to 40% of mice being tumor-free at the end of the study (i.e., day 60 post-tumor challenge) (**Figure 5.1 F**). These mice were monitored for another 40 days (i.e., up to day 100) and were not found to develop any recurrent

Downloaded from jpet.aspetjournals.org at ASPET Journals on April 18, 2024

JPET Fast Forward. Published on October 25, 2018 as DOI: 10.1124/jpet.118.252809
This article has not been copyedited and formatted. The final version may differ from this version.

tumors. Survival analysis revealed that all vaccine regimens resulted in a statistically significant extended survival compared to naïve control, but no significant statistical differences were observed among vaccine regimens (**Figure 5.2**). The median survival times of unvaccinated (naïve) mice and mice vaccinated with a single dose, a prime-boost (on days 0 and 7), or a prime-boost (on days 0 and 21) were 18, 47, 43, and 49 days, respectively.

4. Discussion

Herein, we compared three distinct polyanhydride-based vaccine regimens in terms of: 1) inducing antigen-specific humoral and cellular immune responses; and 2) subsequently protecting against tumor challenge. Side-by-side comparisons of single dose versus two temporally distinct prime-boost regimens involving OVA-loaded 20:80 CPTEG:CPH particles were carried out. We have previously shown that polyanhydride-based particles were capable of stimulating significant OVA-specific cellular immune responses (Wafa et al., 2017) and that, unlike other previously tested polymers which require the presence of a TLR agonist to promote significant cellular immune responses, polyanhydride-based particles have inherent capacity to stimulate TLRs (TLR-2, -4 and -5) (Tamayo et al., 2010). Previously, we have only studied these promising polymers for cancer vaccines in the context of a specific prime-boost regimen (Joshi et al., 2013; Wafa et al., 2017). In this work, we examined the effects of the number, as well as timing, of polyanhydride particle immunizations on antitumor humoral and cellular immune responses.

Analysis of the OVA-release kinetics from the polyanhydride-based particles *in vitro* revealed a burst release (approximately 28% of encapsulated OVA) which likely corresponded to OVA loaded at, or near, the surface of particles. Possible explanations for this observation include: (i) a propensity of the payload to diffuse to the surface, forming

Downloaded from jpet.aspetjournals.org at ASPET Journals on April 18, 2024

JPET Fast Forward. Published on October 25, 2018 as DOI: 10.1124/jpet.118.252809
This article has not been copyedited and formatted. The final version may differ from this version.

a concentration gradient during the fabrication process (during the solvent evaporation step) (Haughney et al., 2013), and/or (ii) water molecules eliminated during the freeze-drying process carrying some of the payload to the surface (Kamaly et al., 2016). The burst release was followed by slow and sustained release of OVA over time, due to the fact that polyanhydride particles predominately degrade through surface erosion (i.e., degradation is limited to the surface) (Katti et al., 2002; Shen et al., 2002; Torres et al., 2006). Assuming that a similar release profile occurs *in vivo,* it is therefore likely that a substantial amount of OVA (50-60%) remained in association with the particles for at least two weeks post-prime and was therefore available for uptake by DCs. This is important since it is widely recognized that delivery of antigen in particulate form (e.g. conjugated to, or encapsulated by, microparticles or nanoparticles) is more likely to stimulate a cellular immune response than antigen in soluble form (Storni et al., 2005; Nembrini et al., 2011). Uptake studies showed that polyanhydride particles were efficiently taken up by BMDCs. DCs exposed to polyanhydride particles demonstrated significant increases in cytokine secretion and CD80/CD86 expression. The expression of these maturation markers contributes to their potency in subsequently activating $CD8^+$ T cells (Acuto and Michel, 2003; Liu et al., 2018). These observations have important implications for developing antitumor responses in hosts with cancer cells.

The efficacy of each vaccine regimen was assessed in terms of cellular and humoral OVA-specific immune responses as well as antitumor activity *in vivo*. Although vaccines for cancer treatment have drawn considerable attention in the past few years (Acres et al., 2004; Guo et al., 2013; Finn, 2014), there is a dearth of data adequately documenting the association between the particle-based cancer vaccine administration strategy and the potency of the subsequent antitumor immune responses. One of the potentially promising outcomes of polymer particle-based vaccines is that they may

Downloaded from jpet.aspetjournals.org at ASPET Journals on April 18, 2024

JPET Fast Forward. Published on October 25, 2018 as DOI: 10.1124/jpet.118.252809
This article has not been copyedited and formatted. The final version may differ from this version.

provide an opportunity for convenient single dose vaccinations, primarily due to their release kinetics. However, most researchers have approached preclinical studies with particle-based vaccines using more conventional prime-boost approaches or without directly comparing temporally distinct prime-boost regimens. Given the vast array of vaccine formulations being generated, it would be of great benefit to understand the ramifications of using different vaccination strategies with different formulations not only in the context of cancer treatment but also in the context of other diseases. In this study, a single dose regimen and two dual dose (prime-boost) vaccine regimens were compared. Administering the booster vaccine dose (irrespective of the time interval) supported the induction of relatively strong OVA-specific antibody (IgG_1-dominated) immune responses in comparison to single dose vaccination which was two orders of magnitude weaker (**Figure 4.2**). Interestingly, prime-boosts were not necessary to generate significant increases in the levels of OVA-specific $CD8^+$ T cells (**Figure 4.1**). Thus, in terms of generating substantive humoral responses using antigen-loaded polyanhydride particles, a prime-boost regimen was required. However, a prime-boost appears to be unnecessary for the enhanced induction of antigen-specific $CD8^+$ T cells. An explanation, albeit speculative, for the findings with respect to humoral responses, is that there was insufficient activation of T-dependent antibody responses when the single dose vaccine was applied, possibly due to limited helper T cell-mediated activation. This may have been due to either insufficient presentation of antigen in the context of MHC class II and/or insufficient TLR stimulation. In other words, the supply of antigen and/or adjuvant (in this case the polymer) may have been limiting in terms of dose and/or duration. Further experiments such as doubling the dosage amount of the single dose vaccine may help determining if such a situation is likely.

Downloaded from jpet.aspetjournals.org at ASPET Journals on April 18, 2024

JPET Fast Forward. Published on October 25, 2018 as DOI: 10.1124/jpet.118.252809
This article has not been copyedited and formatted. The final version may differ from this version.

The prophylactic protection against tumor challenge and overall survival provided by a single dose polyanhydride-based vaccine was comparable to that provided by prime-boost vaccine regimens. These results emphasize the effectiveness of a single dose of the polyanhydride particle-based vaccine in generating significant and enduring cell-mediated immunity as well as protecting against tumor progression. The fact that a single dose vaccination was able to generate an anti-OVA $CD8^+$ T cell response that was sustained until at least day 28 is highly promising. It would be of great value in future experiments to investigate the qualitative nature of the cellular immune responses generated by these particle-based formulations in terms of the generation of central and effector memory T cells. In addition, it would be of interest to observe what effect using these polyanhydride-based vaccines would have in a heterologous vaccination setting. Based on the findings here and combined with the previously reported pathogen-mimicking properties of polyanhydride particles, it appears that these protein-loaded particles have beneficial effects on both B cell and T cell immunity similar to attenuated adenoviruses. If so, these particle-based cancer vaccines may have advantages in terms of clinical applications since issues of safety and neutralizing antibodies would be avoided. Further investigations into heterologous vaccination regimens and qualitative memory T cell responses are future goals. Mechanistically, it is probable that the antitumor effect of the vaccines used here was due, at least in part, to the generation of OVA-specific T cells, however, depletion of various lymphocyte subsets would be required in the future in order to confirm this. Finally, it would also be of interest to investigate the effectiveness of polyanhydride particle-based vaccines and vaccination schedules in the context of a therapeutic model in the presence of immune checkpoint-specific antibodies.

In summary, this study demonstrated that a single vaccination dose of 20:80 CPTEG:CPH polyanhydride particles provided quantitatively similar OVA-specific $CD8^+$ T

Downloaded from jpet.aspetjournals.org at ASPET Journals on April 18, 2024

JPET Fast Forward. Published on October 25, 2018 as DOI: 10.1124/jpet.118.252809
This article has not been copyedited and formatted. The final version may differ from this version.

cell responses and antitumor activities to those generated by prime-boost vaccination regimens. This can potentially obviate the need for a multiple-dose vaccine course of cancer treatment, or at least reduce the number of vaccinations required to achieve effectiveness.

Acknowledgements

We acknowledge support from the Iowa State University Nanovaccine Institute, the Vlasta Klima Balloun Faculty Chair, the National Institutes of Health (1U01CA213862-01A1 and P30 CA086862) and the Lyle and Sharon Bighley Chair of Pharmaceutical Sciences. Authors declare that there is no conflict of interests to disclose.

Author contributions

Participated in research design: Wafa, Geary, Salem.

Conducted experiments: Wafa, Geary, Goodman.

Performed data analysis: Wafa.

Wrote or contributed to the writing of the manuscript: Wafa, Geary, Ross, Narasimhan, Salem.

Downloaded from jpet.aspetjournals.org at ASPET Journals on April 18, 2024

JPET Fast Forward. Published on October 25, 2018 as DOI: 10.1124/jpet.118.252809
This article has not been copyedited and formatted. The final version may differ from this version.

References

Acres B, Paul S, Haegel-Kronenberger H, Calmels B and Squiban P (2004) Therapeutic cancer vaccines. *Curr Opin Mol Ther* **6**:40-47.

Acuto O and Michel F (2003) CD28-mediated co-stimulation: a quantitative support for TCR signalling. *Nat Rev Immunol* **3**:939-951.

Ahmed KK, Geary SM and Salem AK (2014) Applying biodegradable particles to enhance cancer vaccine efficacy. *Immunol Res* **59**:220-228.

Alfarouk KO, Stock CM, Taylor S, Walsh M, Muddathir AK, Verduzco D, Bashir AH, Mohammed OY, Elhassan GO, Harguindey S, Reshkin SJ, Ibrahim ME and Rauch C (2015) Resistance to cancer chemotherapy: failure in drug response from ADME to P-gp. *Cancer Cell Int* **15**:71.

Andersen MH, Schrama D, Thor Straten P and Becker JC (2006) Cytotoxic T cells. *J Invest Dermatol* **126**:32-41.

Behroozi F, Abdkhodaie MJ, Sadeghi Abandansari H, Satarian L, Molazem M, Al-Jamal KT and Baharvand H (2018) Engineering Folate-Targeting Diselenide-containing Triblock Copolymer as a Redox-Responsive Shell-sheddable Micelle for Antitumor Therapy In Vivo. *Acta Biomater*.

Blum JS, Wearsch PA and Cresswell P (2013) Pathways of antigen processing. *Annu Rev Immunol* **31**:443-473.

Colombo BM, Lacave R, Pioche-Durieu C, Masurier C, Lemoine FM, Guigon M and Klatzmann D (2000) Cellular but not humoral immune responses generated by vaccination with dendritic cells protect mice against leukaemia. *Immunology* **99**:8-15.

de Barros CM, Wafa EI, Chitphet K, Ahmed K, Geary SM and Salem AK (2017) Production of Adjuvant-Loaded Biodegradable Particles for Use in Cancer Vaccines. *Methods Mol Biol* **1494**:201-213.

Downloaded from jpet.aspetjournals.org at ASPET Journals on April 18, 2024

JPET Fast Forward. Published on October 25, 2018 as DOI: 10.1124/jpet.118.252809
This article has not been copyedited and formatted. The final version may differ from this version.

Dilnawaz F and Sahoo SK (2018) Augmented Anticancer Efficacy by si-RNA Complexed Drug-Loaded Mesoporous Silica Nanoparticles in Lung Cancer Therapy. *ACS Applied Nano Materials* **1**:730-740.

Finn OJ (2014) Vaccines for cancer prevention: a practical and feasible approach to the cancer epidemic. *Cancer Immunol Res* **2**:708-713.

Fontana F, Liu D, Hirvonen J and Santos HA (2017) Delivery of therapeutics with nanoparticles: what's new in cancer immunotherapy? *Wiley Interdiscip Rev Nanomed Nanobiotechnol* **9**.

Garcia-Cremades M, Pitou C, Iversen PW and Troconiz IF (2017) Characterizing Gemcitabine Effects Administered as Single Agent or Combined with Carboplatin in Mice Pancreatic and Ovarian Cancer Xenografts: A Semimechanistic Pharmacokinetic/Pharmacodynamics Tumor Growth-Response Model. *J Pharmacol Exp Ther* **360**:445-456.

Geary SM, Hu Q, Joshi VB, Bowden NB and Salem AK (2015) Diaminosulfide based polymer microparticles as cancer vaccine delivery systems. *J Control Release* **220**:682-690.

Gomez de Cedron M, Vargas T, Madrona A, Jimenez A, Perez-Perez MJ, Quintela JC, Reglero G, San-Felix A and Ramirez de Molina A (2018) Novel Polyphenols That Inhibit Colon Cancer Cell Growth Affecting Cancer Cell Metabolism. *J Pharmacol Exp Ther* **366**:377-389.

Guo C, Manjili MH, Subjeck JR, Sarkar D, Fisher PB and Wang XY (2013) Therapeutic cancer vaccines: past, present, and future. *Adv Cancer Res* **119**:421-475.

Haughney SL, Petersen LK, Schoofs AD, Ramer-Tait AE, King JD, Briles DE, Wannemuehler MJ and Narasimhan B (2013) Retention of structure, antigenicity, and biological function of pneumococcal surface protein A (PspA) released from polyanhydride nanoparticles. *Acta Biomater* **9**:8262-8271.

Downloaded from jpet.aspetjournals.org at ASPET Journals on April 18, 2024

JPET Fast Forward. Published on October 25, 2018 as DOI: 10.1124/jpet.118.252809
This article has not been copyedited and formatted. The final version may differ from this version.

Irvine DJ, Swartz MA and Szeto GL (2013) Engineering synthetic vaccines using cues from natural immunity. *Nat Mater* **12**:978-990.

Jain JP, Modi S, Domb AJ and Kumar N (2005) Role of polyanhydrides as localized drug carriers. *J Control Release* **103**:541-563.

Joshi VB, Geary SM, Carrillo-Conde BR, Narasimhan B and Salem AK (2013) Characterizing the antitumor response in mice treated with antigen-loaded polyanhydride microparticles. *Acta Biomater* **9**:5583-5589.

Kamaly N, Yameen B, Wu J and Farokhzad OC (2016) Degradable Controlled-Release Polymers and Polymeric Nanoparticles: Mechanisms of Controlling Drug Release. *Chem Rev* **116**:2602-2663.

Katti DS, Lakshmi S, Langer R and Laurencin CT (2002) Toxicity, biodegradation and elimination of polyanhydrides. *Adv Drug Deliv Rev* **54**:933-961.

Lahariya C (2016) Vaccine epidemiology: A review. *J Family Med Prim Care* **5**:7-15.

Li LC, Deng J and Stephens D (2002) Polyanhydride implant for antibiotic delivery--from the bench to the clinic. *Adv Drug Deliv Rev* **54**:963-986.

Liu Y, Wang K-H, Chen H-Y, Li J-R, Laurence TA, Ly S, Liu F-T and Liu G-Y (2018) Periodic Arrangement of Lipopolysaccharides Nanostructures Accelerates and Enhances the Maturation Processes of Dendritic Cells. *ACS Applied Nano Materials* **1**:839-850.

Maher J and Davies ET (2004) Targeting cytotoxic T lymphocytes for cancer immunotherapy. *Br J Cancer* **91**:817-821.

Martinez-Lostao L, Anel A and Pardo J (2015) How Do Cytotoxic Lymphocytes Kill Cancer Cells? *Clin Cancer Res* **21**:5047-5056.

Nembrini C, Stano A, Dane KY, Ballester M, van der Vlies AJ, Marsland BJ, Swartz MA and Hubbell JA (2011) Nanoparticle conjugation of antigen enhances cytotoxic T-cell responses in pulmonary vaccination. *Proc Natl Acad Sci U S A* **108**:E989-997.

Downloaded from jpet.aspetjournals.org at ASPET Journals on April 18, 2024

JPET Fast Forward. Published on October 25, 2018 as DOI: 10.1124/jpet.118.252809
This article has not been copyedited and formatted. The final version may differ from this version.

Paci A, Veal G, Bardin C, Leveque D, Widmer N, Beijnen J, Astier A and Chatelut E (2014) Review of therapeutic drug monitoring of anticancer drugs part 1--cytotoxics. *Eur J Cancer* **50**:2010-2019.

Perry J, Chambers A, Spithoff K and Laperriere N (2007) Gliadel wafers in the treatment of malignant glioma: a systematic review. *Curr Oncol* **14**:189-194.

Reuschenbach M, von Knebel Doeberitz M and Wentzensen N (2009) A systematic review of humoral immune responses against tumor antigens. *Cancer Immunol Immunother* **58**:1535-1544.

Roy J, Adili R, Kulmacz R, Holinstat M and Das A (2016) Development of Poly Unsaturated Fatty Acid Derivatives of Aspirin for Inhibition of Platelet Function. *J Pharmacol Exp Ther* **359**:134-141.

Shen E, Kipper MJ, Dziadul B, Lim MK and Narasimhan B (2002) Mechanistic relationships between polymer microstructure and drug release kinetics in bioerodible polyanhydrides. *J Control Release* **82**:115-125.

Siegel RL, Miller KD and Jemal A (2017) Cancer Statistics, 2017. *CA Cancer J Clin* **67**:7-30.

Siegrist C-A (2013) 2 - Vaccine immunology A2 - Plotkin, Stanley A, in *Vaccines (Sixth Edition)* (Orenstein WA and Offit PA eds) pp 14-32, W.B. Saunders, London.

Storni T, Kundig TM, Senti G and Johansen P (2005) Immunity in response to particulate antigen-delivery systems. *Adv Drug Deliv Rev* **57**:333-355.

Tamayo I, Irache JM, Mansilla C, Ochoa-Reparaz J, Lasarte JJ and Gamazo C (2010) Poly(anhydride) nanoparticles act as active Th1 adjuvants through Toll-like receptor exploitation. *Clin Vaccine Immunol* **17**:1356-1362.

Tian F, Dahmani FZ, Qiao J, Ni J, Xiong H, Liu T, Zhou J and Yao J (2018) A targeted nanoplatform co-delivering chemotherapeutic and antiangiogenic drugs as a tool to reverse multidrug resistance in breast cancer. *Acta Biomater*.

Downloaded from jpet.aspetjournals.org at ASPET Journals on April 18, 2024

JPET Fast Forward. Published on October 25, 2018 as DOI: 10.1124/jpet.118.252809
This article has not been copyedited and formatted. The final version may differ from this version.

Torres MP, Determan AS, Anderson GL, Mallapragada SK and Narasimhan B (2007) Amphiphilic polyanhydrides for protein stabilization and release. *Biomaterials* **28**:108-116.

Torres MP, Vogel BM, Narasimhan B and Mallapragada SK (2006) Synthesis and characterization of novel polyanhydrides with tailored erosion mechanisms. *J Biomed Mater Res A* **76**:102-110.

Wafa EI, Geary SM, Goodman JT, Narasimhan B and Salem AK (2017) The effect of polyanhydride chemistry in particle-based cancer vaccines on the magnitude of the anti-tumor immune response. *Acta Biomater* **50**:417-427.

Wang Y, Qiao S-L and Wang H (2018) Facile Synthesis of Peptide Cross-Linked Nanogels for Tumor Metastasis Inhibition. *ACS Applied Nano Materials* **1**:785-792.

Zhang L, Wang W and Wang S (2015) Effect of vaccine administration modality on immunogenicity and efficacy. *Expert Rev Vaccines* **14**:1509-1523.

Zhou J, You W, Sun G, Li Y, Chen B, Ai J and Jiang H (2016) The Marine-Derived Oligosaccharide Sulfate MS80, a Novel Transforming Growth Factor beta1 Inhibitor, Reverses Epithelial Mesenchymal Transition Induced by Transforming Growth Factor-beta1 and Suppresses Tumor Metastasis. *J Pharmacol Exp Ther* **359**:54-61.

Downloaded from jpet.aspetjournals.org at ASPET Journals on April 18, 2024

JPET Fast Forward. Published on October 25, 2018 as DOI: 10.1124/jpet.118.252809
This article has not been copyedited and formatted. The final version may differ from this version.

Legends for Figures

Fig. 1: Chemical structure of 20:80 CPTEG:CPH polyanhydride copolymer.

Fig. 2.1: SEM images of 20:80 CPTEG:CPH polyanhydride particles. (A): OVA-loaded particles; (B): C6-loaded particles; (C): empty particles. Scale bar represents 1 μm.

Fig. 2.2: Cumulative *in vitro* release of OVA from 20:80 CPTEG:CPH polyanhydride particles. (A) Percent OVA release over time; (B) Linear regression with 95% confidence interval, excluding the data points of the first day. Data points are plotted as mean ± SD.

Fig. 3.1: *In vitro* BMDC stimulation with, and uptake of, polyanhydride particles. (A): CD80/CD86 expression on cell surface (flow cytometry) of BMDCs and (B) IL-10 and IL-12p70 concentrations in the cell culture supernatants (ELISA) after 24-hr incubation with empty polyanhydride particles. (C): uptake study by BMDCs of C6-loaded polyanhydride particles at two-time points; 1 and 4 hrs.

Fig. 3.2: Uptake of C6-loaded polyanhydride particles by BMDCs. (A): untreated BMDCs; (B): BMDCs treated with C6-loaded polyanhydride particles. Scale bar represents 20 μm.

Fig. 4.1: Percentage of OVA-specific $CD8^+$ T cells in the peripheral blood of mice vaccinated with different polyanhydride-based vaccine regimens. The percentage of OVA-specific $CD8^+$ T cells was measured at two-time points: (A) two weeks (data from single dose and prime-boost 0/21 groups were combined since mice in both group received only one dose) and (B) four weeks post-prime vaccination. Data are plotted as mean ± SEM. $**^n p<0.01$. Superscript n = compared with naïve group.

Fig. 4.2: OVA-specific IgG_1 and IgG_{2C} serum titers in mice vaccinated with different polyanhydride-based vaccine regimens. Data are plotted as mean ± SEM. $***^n p<0.001$. Superscript n = compared with naïve group.

Downloaded from jpet.aspetjournals.org at ASPET Journals on April 18, 2024

JPET Fast Forward. Published on October 25, 2018 as DOI: 10.1124/jpet.118.252809
This article has not been copyedited and formatted. The final version may differ from this version.

Fig. 5.1: Prophylactic antitumor effect of vaccinating mice with different polyanhydride-based vaccine regimens. Mice were vaccinated as indicated and subsequently challenged with E.G7-OVA cells 35 days post prime. (A-D) Each curve represents the tumor growth for each individual mouse. (E) Average tumor volume (data are plotted as mean ± SEM): naïve (♦); single dose regimen (■); prime-boost (0/7) regimen (▲); prime-boost (0/21) regimen (●). (F) Percent tumor-free mice on days 16 (last day that all naïve mice were alive) and 60 (end of study) post-tumor challenge.

Fig. 5.1: Survival curve of prophylactically vaccinated mice subsequently challenged with E.G7-OVA cells. Prior to tumor challenge, mice were vaccinated with polyanhydride-based particles with indicated regimens. $^{**n}p<0.01$, $^{***n}p<0.001$. Superscript n = compared with naïve group.

Downloaded from jpet.aspetjournals.org at ASPET Journals on April 18, 2024

JPET Fast Forward. Published on October 25, 2018 as DOI: 10.1124/jpet.118.252809
This article has not been copyedited and formatted. The final version may differ from this version.

Tables

Table 1: Properties of polyanhydride particles.

	OVA-loaded particles	C6-loaded particles	Empty particles
Particle Size (d.nm)	959 ± 20	913 ± 22	926 ± 17
Polydispersity Index (PDI)	0.17 ± 0.04	0.12 ± 0.02	0.03 ± 0.01
Zeta Potential (mV)	–31.3 ± 2.8	–26.5 ± 0.2	–26.1 ± 0.2
Loading Capacity (µg per mg of particles)	6.0 ± 0.2	0.74 ± 0.02	-
Encapsulation Efficiency (%)	28.0 ± 0.9	73.9 ± 1.6	-

Data are presented as mean ± SD.

Downloaded from jpet.aspetjournals.org at ASPET Journals on April 18, 2024

JPET Fast Forward. Published on October 25, 2018 as DOI: 10.1124/jpet.118.252809
This article has not been copyedited and formatted. The final version may differ from this version.

Figures

Fig. 1

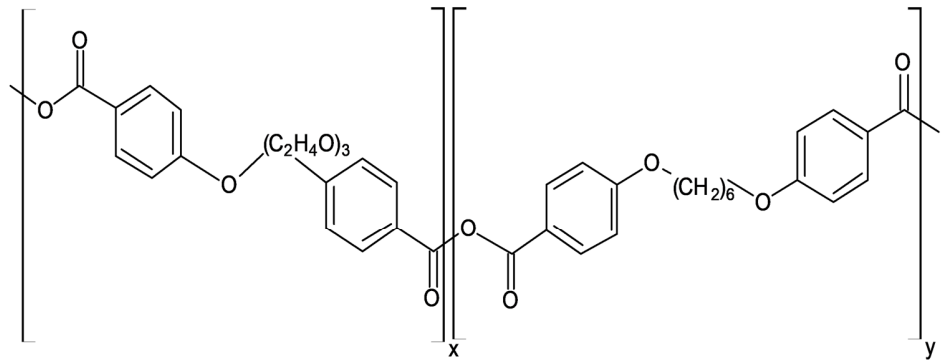

Downloaded from jpet.aspetjournals.org at ASPET Journals on April 18, 2024

JPET Fast Forward. Published on October 25, 2018 as DOI: 10.1124/jpet.118.252809
This article has not been copyedited and formatted. The final version may differ from this version.

Fig. 2.1

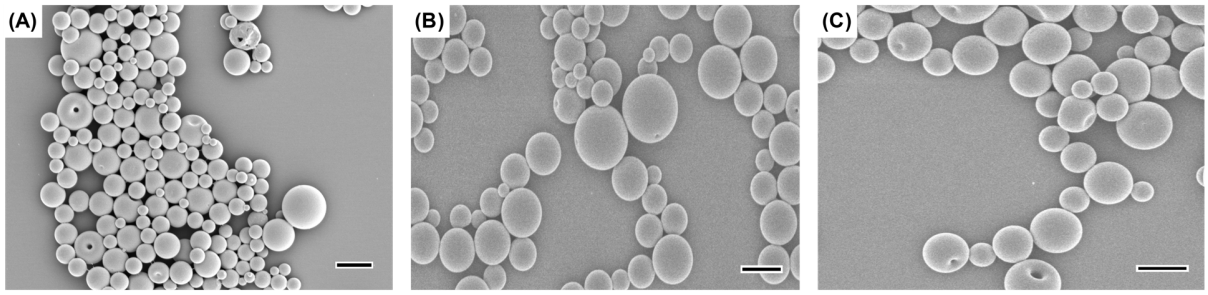

Downloaded from jpet.aspetjournals.org at ASPET Journals on April 18, 2024

JPET Fast Forward. Published on October 25, 2018 as DOI: 10.1124/jpet.118.252809
This article has not been copyedited and formatted. The final version may differ from this version.

Fig. 2.2

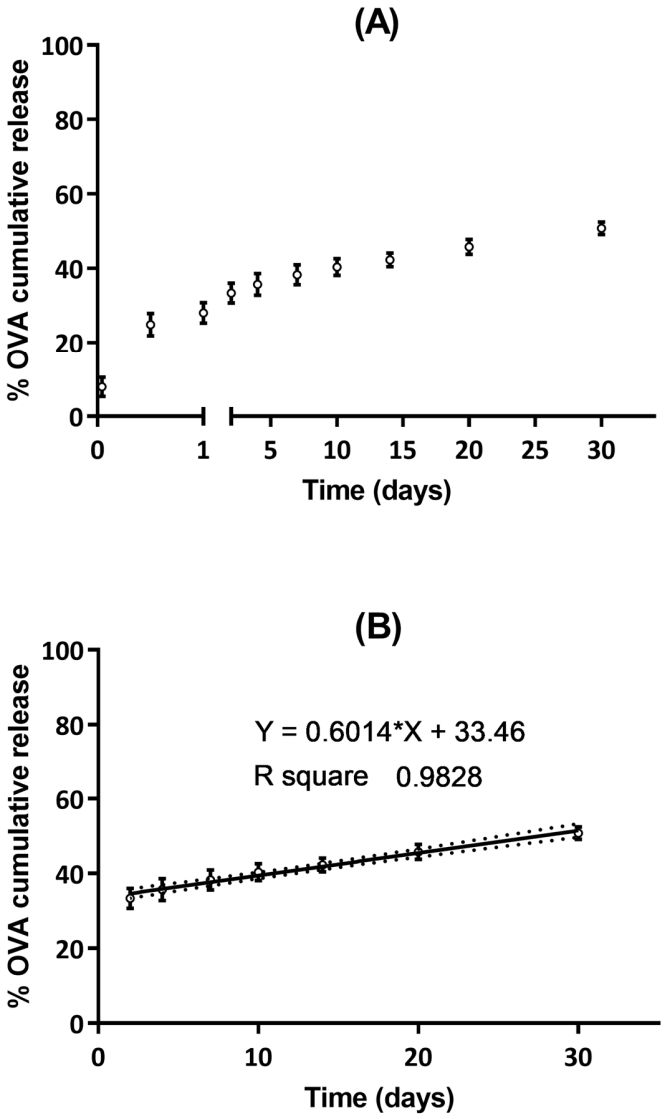

Downloaded from jpet.aspetjournals.org at ASPET Journals on April 18, 2024

JPET Fast Forward. Published on October 25, 2018 as DOI: 10.1124/jpet.118.252809
This article has not been copyedited and formatted. The final version may differ from this version.

Fig. 3.1

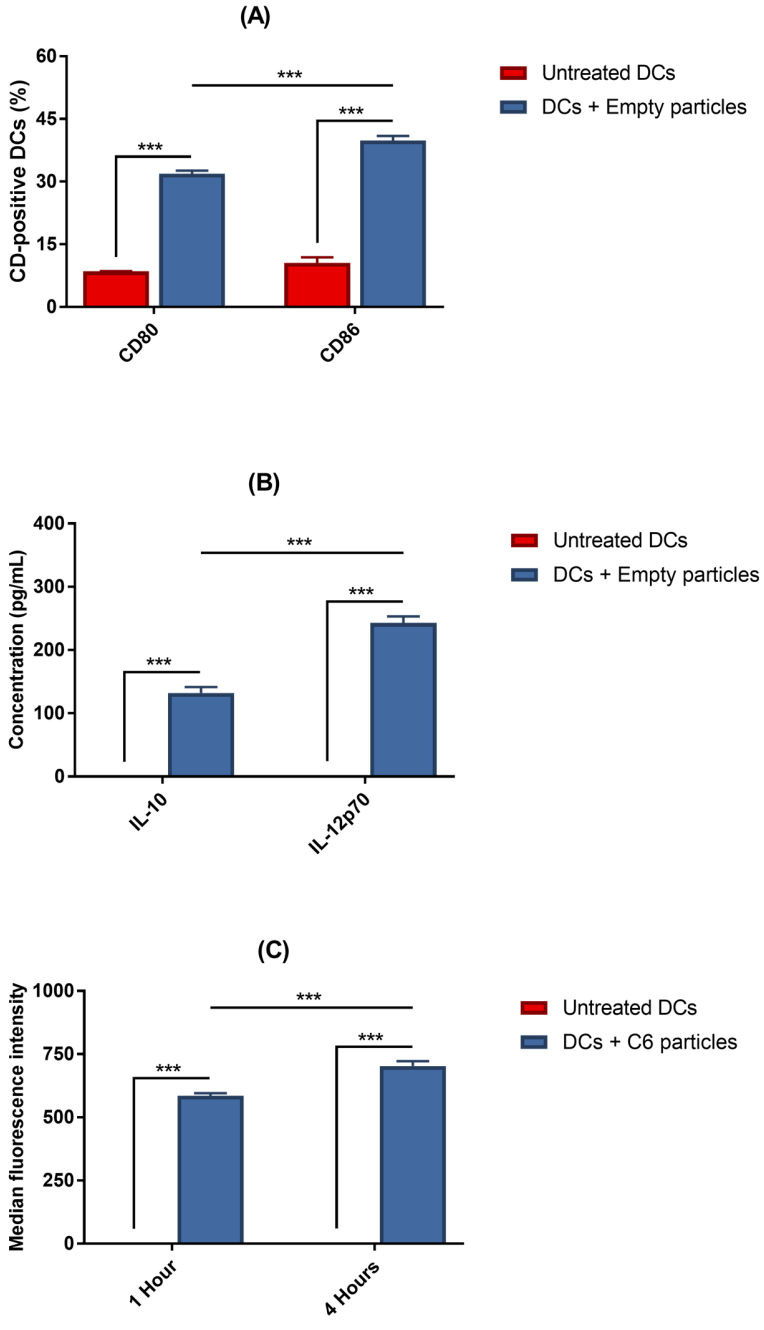

Downloaded from jpet.aspetjournals.org at ASPET Journals on April 18, 2024

JPET Fast Forward. Published on October 25, 2018 as DOI: 10.1124/jpet.118.252809
This article has not been copyedited and formatted. The final version may differ from this version.

Fig. 3.2

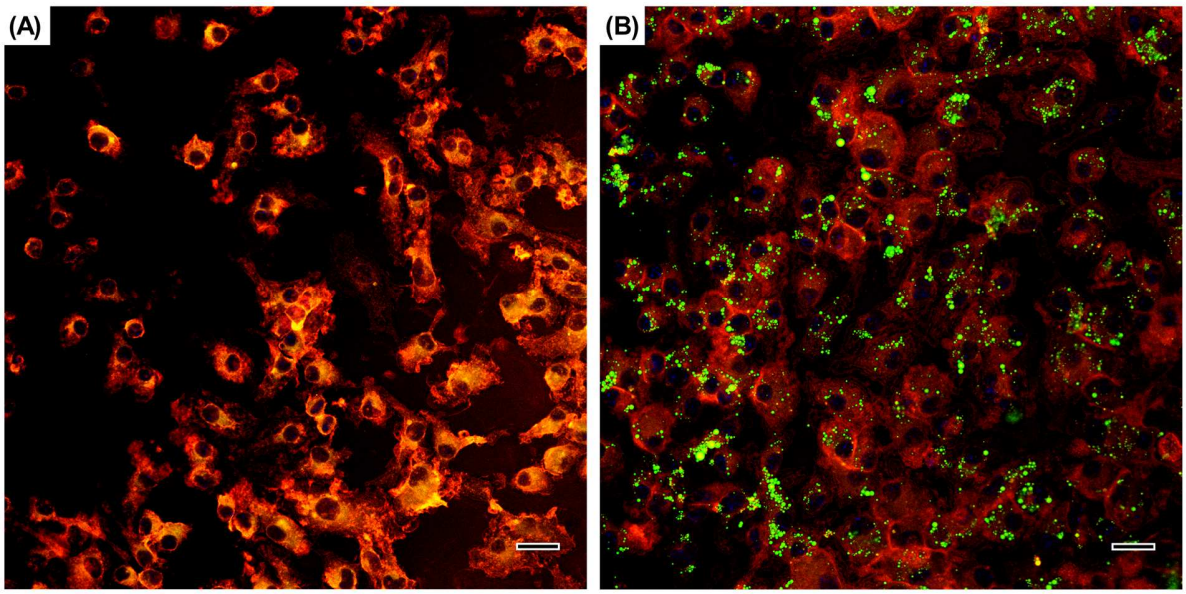

Downloaded from jpet.aspetjournals.org at ASPET Journals on April 18, 2024

JPET Fast Forward. Published on October 25, 2018 as DOI: 10.1124/jpet.118.252809
This article has not been copyedited and formatted. The final version may differ from this version.

Fig. 4.1

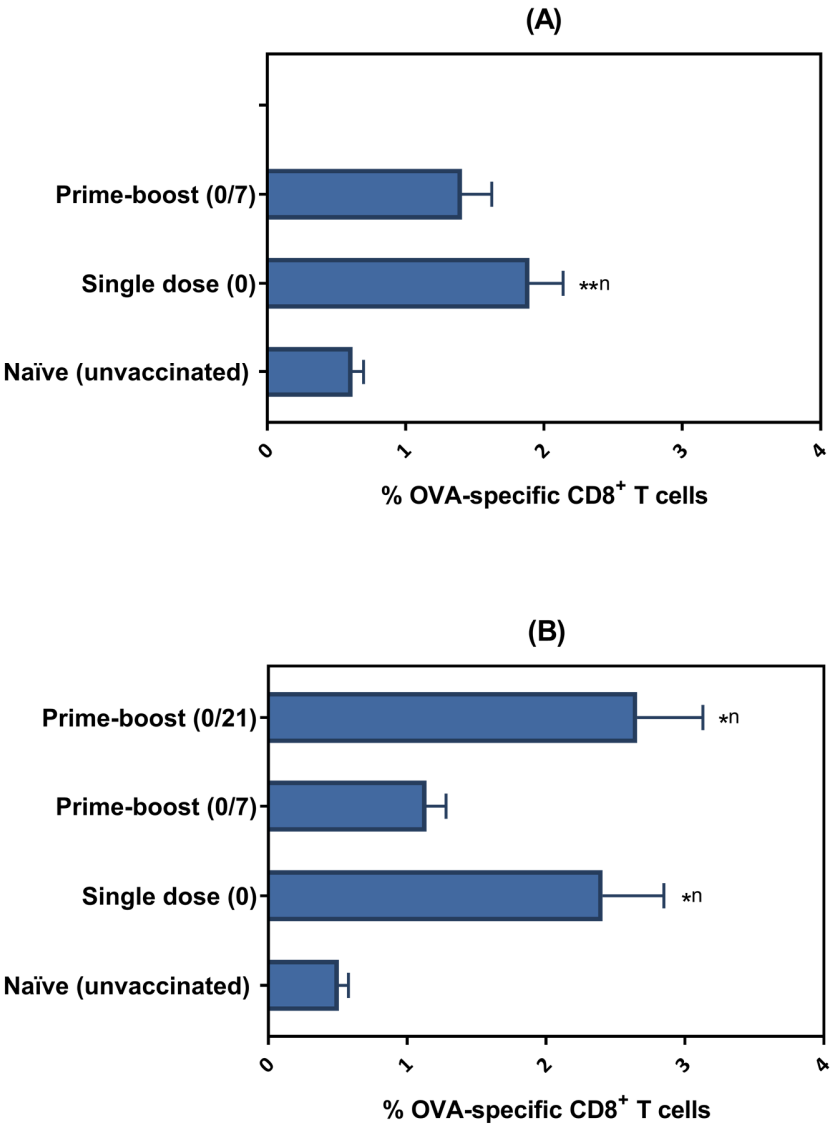

Downloaded from jpet.aspetjournals.org at ASPET Journals on April 18, 2024

JPET Fast Forward. Published on October 25, 2018 as DOI: 10.1124/jpet.118.252809
This article has not been copyedited and formatted. The final version may differ from this version.

Fig. 4.2

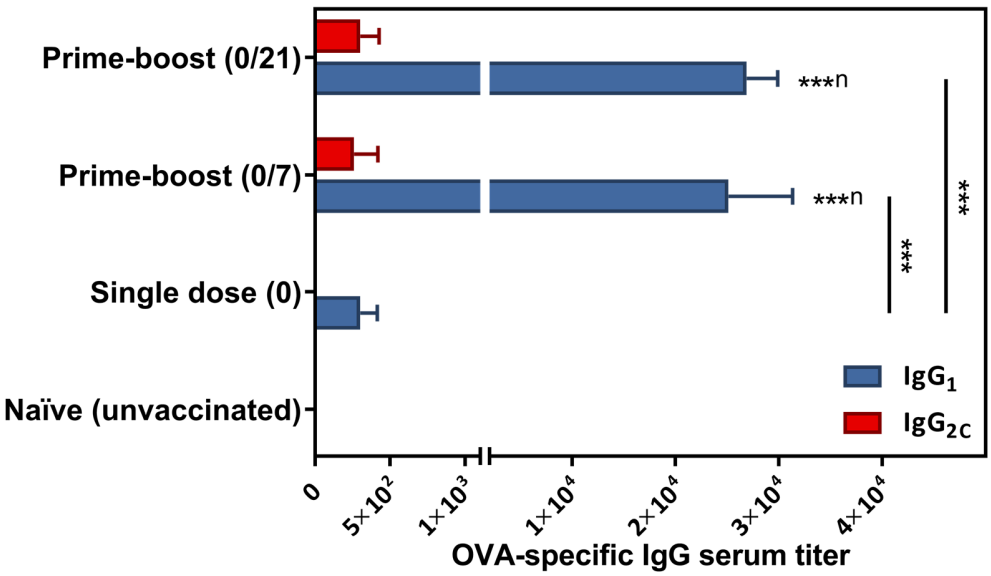

Downloaded from jpet.aspetjournals.org at ASPET Journals on April 18, 2024

Fig. 5.1

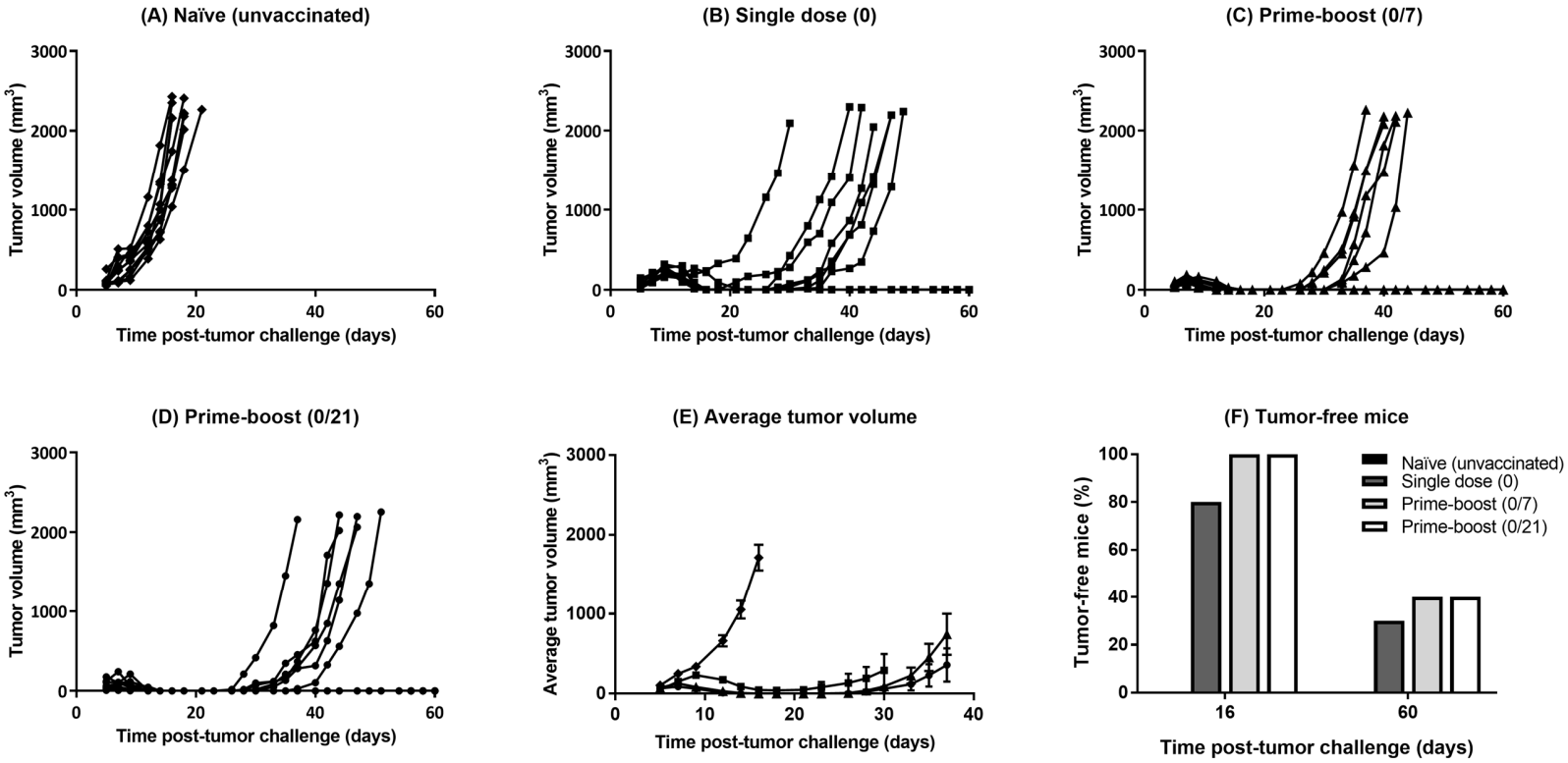

JPET Fast Forward. Published on October 25, 2018 as DOI: 10.1124/jpet.118.252809
This article has not been copyedited and formatted. The final version may differ from this version.

Downloaded from jpet.aspetjournals.org at ASPET Journals on April 18, 2024

JPET Fast Forward. Published on October 25, 2018 as DOI: 10.1124/jpet.118.252809
This article has not been copyedited and formatted. The final version may differ from this version.

Fig. 5.2

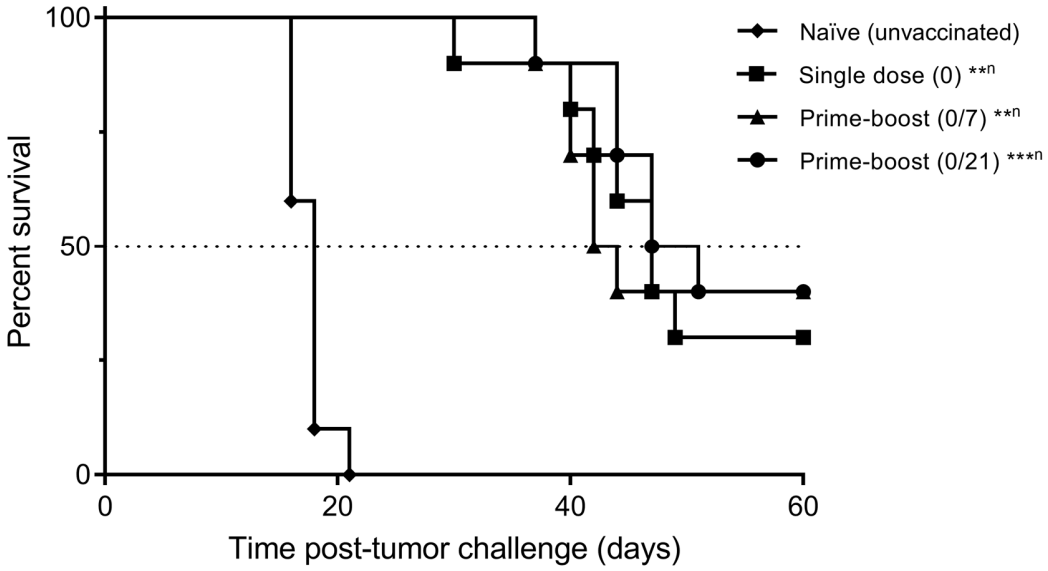

Downloaded from jpet.aspetjournals.org at ASPET Journals on April 18, 2024